2026 IEEE International Conference on Robotics and Automation (ICRA 2026)
June 1-5, 2026. Vienna, Austria

Enabling automated and personalized motor assessment in neurorehabilitation: generating patient-specific reference movements with a Virtual Humanoid Twin

Mathilde Legrand[1,2], Olivier Lambercy[2] and Roger Gassert[2]

Abstract— **Recovering upper-limb motor functions impaired by trauma or neurological disease is a long and challenging process. To monitor a patient's progress through the various stages of rehabilitation and guide therapy, regular movement assessment is essential. However, such evaluations are rarely conducted in clinical practice due to time constraints and the need for cumbersome equipment. A key limitation is the access to reference motion data, typically derived from averaged movements of unimpaired individuals, which requires new data collection for each task and lacks personalization (e.g., accounting for individual morphology or motor abilities).**
We present a novel method to generate patient-specific reference motions directly from the patient's hand pose using a personalized model of the patient, the Virtual Humanoid Twin (VHT). By solving an ergonomic-based optimal control problem, our approach produces tailored reference motions without prior task-specific data. We validated this method on two motor tasks (reaching and pouring) using data from seven unimpaired participants, with and without an elbow orthosis restricting motion. Analysis of joint trajectories, range of motion, and normalized multi-dimensional Dynamic Time Warping confirmed that VHT-generated motions were more ergonomic than those with the orthosis and closely matched natural movements. The method's rapid generation time can also enable real-time reference motion estimation, parallel to the patient's movements. This innovation simplifies access to reference motions while providing personalization. It creates opportunities for automated motor assessment in neurorehabilitation, enhancing patient recovery tracking through regular evaluations.

I. INTRODUCTION

Life can be a real challenge when motor functions are reduced, due to neurological diseases or after a traumatic accident for instance. Grasping an object and other simple daily life tasks become arduous, which reduces the autonomy of affected people and their quality of life [1], [2]. Motor rehabilitation is crucial to help people recover mobility and, with mobility, to recover independence [3]. Throughout this long process, motion assessment is key: to precisely evaluate the initial impairment, to give therapists up-to-date information to adapt the rehabilitation program and to follow patient progress, which can boost patient motivation. Numerous methods exist to assess human motions in a clinical context, from visual assessments, that rely on the therapist's expertise, to more quantitative and objective measures, including clinical scores, kinematic metrics or robotic tools [4], [5], [6]. For the latter, a clear consensus on assessment protocols and outcome measures is still a work in progress [7], [8]. Evaluating one's motor abilities, however, is time-consuming and is often only performed at the beginning and at the end of the rehabilitation process. Recent works have thus developed methods to automatize assessments [9], [10]. While the latter show promise for easier and faster motor assessment, they focus on clinical scores and global statements. We also need to evaluate full motions and joint trajectories for more in-depth assessment [6] and the automation of such detailed motion analysis remains lacking.

Movement evaluation typically relies on comparing a patient's performance to a reference, either subconsciously integrated by the therapist or derived from averaged normative data collected from unimpaired people [11]. The collection of these data is laborious: a large number of participants have to be recorded to counter the natural variability of human motions [12], and each new task to assess demands its dedicated reference dataset. For upper-limb motions, which are inherently very diverse, it is thus nearly impossible to objectively evaluate joint trajectories in clinical routine. The time and specialized equipment needed to gather task-specific reference data are often prohibitive for clinicians. To enable automated and detailed motion evaluations and better track patient's recovery during rehabilitation, we need a method to access reference data that (i) does not require a multi-participant data collection and (ii) can be easily adapted to any task. Moreover, using a global average of unimpaired motion data as reference is not necessarily meaningful because it severely lacks personalization. While the patient's morphology is a significant factor impacting motion [13], [14] that is omitted with averaging, one may also question the relevance of assuming all joints as fully movable for the patient as some can have permanent mobility limitations [15], [16]. Consequently, unimpaired reference data may not represent an achievable or meaningful goal for many patients. With this in mind, we here present an original approach to respond to these important needs and enhance upper-limb motor assessment during rehabilitation: we suggest to generate (instead of collecting) reference data with a personalized biomechanical model of the patient,

*This work was supported by the ETH Zurich Postdoctoral Fellowship program

[1]Mathilde Legrand is with GIPSA-lab Grenoble Images Parole Signal Automatique, Univ. Grenoble Alpes, CNRS, Grenoble INP, GIPSA-lab, 38000 Grenoble, France mathilde.lestoille@gipsa-lab.fr

[2]Mathilde Legrand, Olivier Lambercy and Roger Gassert are with the Rehabilitation Engineering Laboratory, Department of Health Sciences and Technology, ETH Zurich, 8092 Zurich, Switzerland olivier.lambercy@hest.ethz.ch, roger.gassert@hest.ethz.ch

called the virtual humanoid twin (VHT). The purpose of this approach is to provide easy and non-task-specific access to reference data for detailed motor assessments (e.g., joint trajectories) during neurorehabilitation. This, in turn, opens the door to automated -and thus regular- motion evaluations. Rapid and impressive progress has been made in human motion generation, originally with optimal control theory [17], [18], [19], and more recently with generative models [20], [21]. Optimal control methods can accurately simulate or reproduce motions from unimpaired subjects but each method is tailored to a precise task [19], [22]. Generative models are less specific: physically realistic motions can be generated for several tasks, but task success is still not guaranteed and the simulation time is in the range of hours [20], [21], which prohibits clinical use. In our work, we take a novel approach to generate reference motions with the VHT. We propose to take advantage of the robustness and the execution speed of optimal control but with a new framework, inspired by how physiotherapists guide their patient during rehabilitation: our optimization problem is primarily defined with ergonomic rules, leading to a formulation that does not depend on the task.

In this paper, we first present the concept of the VHT together with the motion generation method (Section II). To validate our approach, we applied this concept to two different upper-limb motor tasks: reaching and pouring. VHT motions were generated from data collected from seven unimpaired participants performing both tasks with and without an elbow orthosis (Section III). Considering a VHT with full mobility, we expect the VHT motions to be more ergonomic than pseudo-impaired movements (with the orthosis) and ideally close to natural performance, this for both motor tasks without any adaptation of the algorithm. Results are presented Section IV. This study contributes to the establishment of a seamless process for accessing reference data, laying the groundwork for automated detailed movement analysis during rehabilitation. This process eliminates the need for heavy upstream work, while offering the valuable benefit of personalization.

II. Proposed approach

Our VHT approach is based on the following observation: when a therapist guides a patient during a rehabilitation session, the main aim is to avoid compensatory motions, which can induce pain and musculoskeletal disorders [23], [24]. This first involves recovering mobility (with therapy) and then finding an ergonomic motion to perform a task with the available motor functions, that are not necessarily all recovered. Our reference motion generation algorithm thus aims at optimizing the patient's movement configuration during the task, through the minimization of an ergonomic cost. An important assumption in this approach is that the patient always manages to perform the task [23], i.e., the hand pose (position and orientation) is considered as correct, but the adopted body pose is incorrect (due to affected motor functions). This is inspired by [25], where a static method was developed to evaluate whether a robotic prosthesis was correctly positioned at the end of a manipulation task. In the present work, we consider a quasi-static approach: while following the patient's hand pose, the body configuration of the patient is optimized at each frame of the evaluated task. Depending on the execution time of the optimization step, this can give the opportunity to generate reference motions during the execution of the task by the patient.

Virtual Humanoid Twin: the VHT is the basic building block of our approach. It represents the patient as a kinematic chain, with an adjustable number of degrees of freedom (DoF), depending on the application. In this paper, we considered upper-limb tasks, for which the patient is seated, and thus included the upper body only. The VHT consists of a kinematic chain with 19 DoF: two for the lumbar spine, three for the trunk, three for the shoulders, two for the elbows and two for the wrists (see Figure 1). The dimensions of the VHT are defined with the anatomical attributes of each patient, identified during a calibration step. The motor capacities of the VHT (e.g., joint range of motions) can also be personalized to the patient.

Reference motion generation algorithm: the VHT is characterized by a vector of joint angles $\mathbf{q} = (q_i), i \in \{1...n\}$ with n the number of DoF of the kinematic model. At each time frame t, we aim to compute $\hat{\mathbf{q}}_t$, the optimized body configuration of the patient, that results in the same hand pose as the patient but with a more ergonomic configuration. We thus assume that a sensing system provides a measure of the patient's hand pose at any time t. $\hat{\mathbf{q}}_t$ is defined by:

$$\hat{\mathbf{q}}_t = \underset{\mathbf{q}}{\operatorname{argmin}}\, C(\mathbf{q}, \alpha) \text{ s.t. } \begin{cases} \mathbf{h}(\mathbf{q}) = \mathbf{h}_p \\ \mathbf{q}^- \leq \mathbf{q} \leq \mathbf{q}^+ \end{cases} \quad (1)$$

with C an ergonomic cost function, α a potential list of additional parameters characterizing the ergonomic cost, $\mathbf{h}$ the kinematic function mapping the joint vector $\mathbf{q}$ into the hand pose, $\mathbf{h}_p$ the current hand pose of the patient given by the sensing system, $\mathbf{q}^-$ and $\mathbf{q}^+$ lower and upper boundaries for joint angles. For the cost function C, we simply choose:

$$C(\mathbf{q}, \mathbf{q}_d, \mathbf{q}_{t-1}) = ||\mathbf{K}(\mathbf{q} - \mathbf{q}_d)||_2^2 + 0.01 \times ||\mathbf{q} - \mathbf{q}_{t-1}||_2^2 \quad (2)$$

with $\mathbf{K} \in \mathbb{R}_+^{n \times n}$ a diagonal matrix of positive weights, $\mathbf{q}_d$ a desired ergonomic configuration and $\mathbf{q}_{t-1}$ the VHT configuration of the previous time frame. The matrix $\mathbf{K}$ allows to tune the ergonomic significance of each joint since, as shown in ergonomic scores such as the Rapid Upper Limb Assessment (RULA) [26], not all joints play a similar ergonomic role. The trunk, for instance, has a higher cost than the shoulder. $\mathbf{q}_d$ was defined as the rest posture of the human before the beginning of the task, considered as ergonomic. The second part of C ensures a smooth transition between time frames.

III. Materials and Methods

A. Experimental set-up

To validate the proposed approach, we tested the VHT framework on a reaching task which consisted in reaching three predefined positions on a table with a glass in the hand, from a fixed starting position (see Figure 2a). The

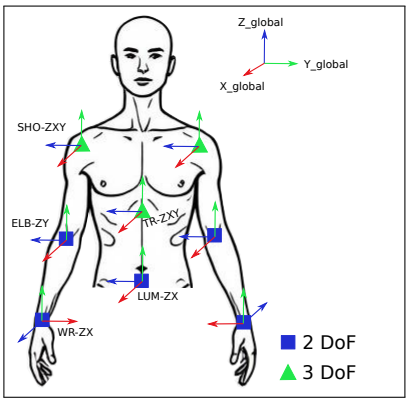

Fig. 1: Virtual humanoid twin (VHT): kinematic chain representing the patient, with individual anatomical attributes. Model used for the application case of this paper. The joint abbreviations are: LUM for lumbar spine, TR for trunk, SHO for shoulder, ELB for elbow and WR for wrist

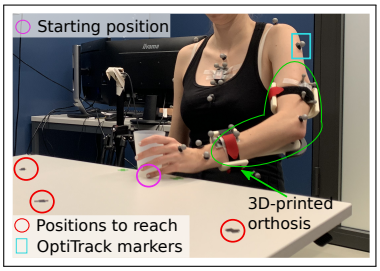

(a) Reaching task, *Impaired* condition.

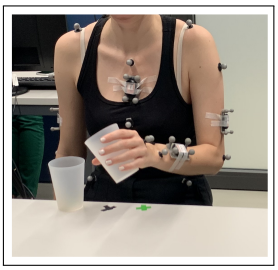

(b) Pouring task, *Natural* condition.

Fig. 2: Experimental set-up for the data collection of two upper-limb tasks: (a) reaching and (b) pouring. Optical motion capture was used to record participants' motions. The tasks were performed with and without a 3D-printed orthosis limiting the elbow joint to 90 $\pm$ 10 deg, to mimic loss of motor functions.

target positions were adapted to correspond to 80% of the participants' arm length. Seven unimpaired adults (mean age 27$\pm$3 years), with no history of neurological, orthopedic or rheumatologic disease which would affect upper body functions, performed this task in two conditions: first naturally and second while wearing a 3D-printed orthosis that limited the elbow joint at 90 $\pm$ 10 deg (see Figure 2a). The first condition, later called *Natural*, was collected to obtain a ground truth for the evaluation of the reference motion generation. The second condition, later called *Impaired*, allowed to collect pseudo-impaired motions that mimicked patients: the orthosis affected motor functions and induced non-ergonomic movements from the participants, such as compensations with the trunk. Four repetitions (with one repetition consisting in reaching the three targets) were performed per condition. All participants performed the task with the right arm; the left arm was kept straight along the body. To test the generalization of the VHT approach on a second task, four participants also performed a pouring task which consisted in transferring an imagined liquid from one glass to another (see Figure 2b). The pouring task was also performed four times for the two conditions, with the right arm. Motion data were recorded at 120Hz with the optical motion capture OptiTrack (OptiTrack NaturalPoint Inc., USA). Reflecting markers were positioned on participants' upper body following the Plug-in Gait upper body model [27]. This study was approved by the ETH Zurich ethics committee (No 2022-N-195). All participants gave their informed consent, in accordance with the Declaration of Helsinki.

B. Data processing and analysis

The same processing and analysis were conducted for both the reaching and the pouring tasks. After collection, the motion data were post-processed with Motive (Motive OptiTrack NaturalPoint Inc., USA): missing time points in marker trajectories were filled with polynomial or linear interpolation. When marker data were not good enough (bad visibility for required markers), the repetition was not included in the analysis (1/56 for reaching and 4/32 for pouring). The data were then exported to Python 3.9 and filtered with a low-pass butterworth filter, with a cut-off frequency of 10Hz. The calibration of the VHT and the reference motion generation were then conducted off-line. All markers were used to calibrate the VHT model for each participant and define the desired ergonomic configuration $\mathbf{q}_d$ (rest position). The VHT was calibrated on the starting position using the data preceding the first repetition of each task: markers were used to retrieve the joint centers, allowing in a second step to scale the VHT model to each participant. In this study, a reduced biomechanical model was used, including the lumbar spine, the trunk and the right arm but not the left arm, which was kept along the body. The data of hand and wrist markers of the right arm were used to measure $\mathbf{h}_p$, the hand pose of the participants, during the entire motion.

To evaluate the reference motion generation algorithm, we first checked that the VHT indeed performed the same task as the participants, i.e., correctly followed their hand pose, looking at the Root Mean Square Error (RMSE) between the trajectories of the participants' hand and wrist markers and those of the VHT. We then compared joint trajectories of the participants with the ones generated with the VHT. Participants' joint trajectories were computed for each repetition with inverse kinematics, using the biomechanical model of the VHT to recover the joint angles best matching the markers. Besides joint trajectories, we computed the Range of Motion (ROM) of each DoF and the normalized, multi-dimensional Dynamic Time Warping (md-DTW) distance. The DTW distance was obtained with the dtw package [28], [29], with the *symmetric2* step pattern and normalization, as described in [28]. It was computed between the second *Natural* repetition of the participant and every other condition (*Natural* and *Impaired* repetitions of the participants and of the VHT). The second *Natural* repetition was selected instead of the first one to avoid any discovery effect. The

multi-dimensional DTW distance is then the sum of the DTW distances of each DoF [30]. The ROM was averaged over repetitions and over participants while individual values were kept for md-DTW distance. The execution time of the optimization step was saved, in order to evaluate the possibility of generating reference motions with the VHT simultaneously to the participant. No statistics were conducted due to the small number of participants.

C. VHT motion generation

The ergonomic optimization to generate VHT motions based on each participant's movement was implemented on Python 3.9, using the Pinocchio library [31] and CasADi [32] with IPopt solver to solve the optimization problem. To reduce the number of sensors and the data processing required to obtain the hand pose to a minimum, we defined $\mathbf{h}(\mathbf{q})$ as

$$\mathbf{h}(\mathbf{q}) = \begin{pmatrix} \mathbf{m}_h \\ \mathbf{m}_{w1} \\ \mathbf{m}_{w_2} \end{pmatrix} \tag{3}$$

with $\mathbf{m}_h$, $\mathbf{m}_{w1}$, $\mathbf{m}_{w2}$ being the 3D position vectors of the hand and the two wrist markers respectively. To avoid defining an unsolvable problem due to too hard equality constraints, we adapted Equation (1) and modified the equality constraint into inequality constraints as follows:

$$\hat{\mathbf{q}}_t = \underset{\mathbf{q}}{\operatorname{argmin}}\, C(\mathbf{q}, \mathbf{q}_d, \mathbf{q}_{t-1}) \text{ s.t. } \begin{cases} \mathbf{h}_p^- \leq \mathbf{h}(\mathbf{q}) \leq \mathbf{h}_p^+ \\ \mathbf{q}^- \leq \mathbf{q} \leq \mathbf{q}^+ \end{cases} \tag{4}$$

with $\mathbf{h}_p^- = \begin{pmatrix} 0.99\,\mathbf{m}_{h,p} \\ 0.95\,\mathbf{m}_{w1,p} \\ 0.95\,\mathbf{m}_{w_2,p} \end{pmatrix}$ and $\mathbf{h}_p^+ = \begin{pmatrix} 1.01\,\mathbf{m}_{h,p} \\ 1.05\,\mathbf{m}_{w1,p} \\ 1.05\,\mathbf{m}_{w_2,p} \end{pmatrix}$. The matrix $\mathbf{K}$ of ergonomic weights was defined based on the RULA score: $\mathbf{K} = diag([\sqrt{300}, \sqrt{300}, \sqrt{100}, \sqrt{100}, \sqrt{20}, 0, \sqrt{20}, 0, 0, \sqrt{10}, \sqrt{5}, 0])$.

In this work, the VHT was always assigned full mobility, which means, from a clinical point of view, that we assumed the participants to be able to recover all their motor functions with rehabilitation. The lower and upper boundaries for joint angles, $\mathbf{q}^-$ and $\mathbf{q}^+$, were thus defined based on unimpaired human biomechanical capacities: $\mathbf{q}^- = (-\pi, -\pi/4, -\pi/3, -\pi/3, -\pi/3, -\pi/4, -\pi, -\pi/2, 0, -\pi/10, -\pi/2, -\pi/4)$ and $\mathbf{q}^+ = (\pi/4, \pi/4, \pi/8, \pi/3, \pi/3, 2\pi/3, \pi/3, \pi, 7\pi/8, \pi, \pi/2, \pi/4)$.

VHT motions were generated from movements of the two conditions, *Natural* and *Impaired*. *Impaired* illustrated the real use case of the VHT: reference motions are generated from an impaired movement and we expect to obtain a more ergonomic movement. We also generated motions from unimpaired movements (*Natural* condition) in order to validate that, in this case, the generation algorithm returned joint trajectories similar to the unimpaired ones. For both conditions and both motor tasks, the VHT motion generation used the exact same algorithm. The codes and data are available upon reasonable request.

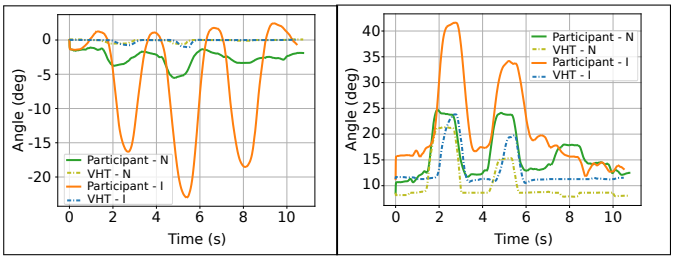

(a) Lumbar flexion (LUMZ). (b) Trunk rotation (TRY).

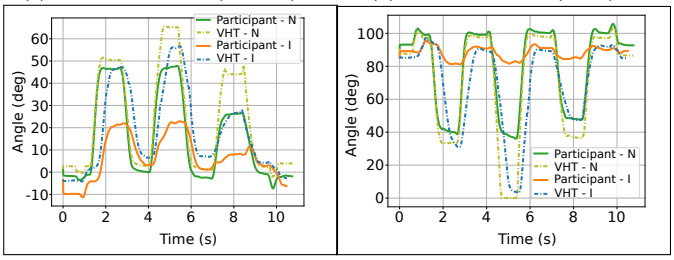

(c) Shoulder flexion (SHOZ). (d) Elbow flexion (ELBZ).

Fig. 3: Examples of real (solid lines) and generated (dotted lines) trajectories for the reaching task, for one participant. Participant - N and Participant - I are the real trajectories of the participant for one *Natural* and one *Impaired* repetition resp.; VHT - N and VHT - I are the trajectories generated from the participant's *Natural* and *Impaired* repetitions resp.

IV. RESULTS

A. Reaching task

The execution time of the optimization step for the reaching task was 40±1ms (25Hz). The RMSE (averaged over repetitions and participants) of the hand and the two wrist markers were similar for the two conditions and equal to 4±0.4mm (*Natural*) and 5±0.7mm (*Impaired*) for the hand, 9±3mm (*Natural*) and 8±2mm (*Impaired*) and 10±3mm (*Natural*) and 10±1mm (*Impaired*) for the wrist.

Fig. 3 shows typical angular trajectories for one participant for the four DoF of the reaching task: the lumbar flexion/extension (LUMZ around local Z axis), the trunk rotation (TRY around local Y axis), the shoulder flexion/extension (SHOZ around local Z axis) and the elbow flexion/extension (ELBZ around local Z axis). In a first step, we can focus on the participant's own motions, with green lines showing one *Natural* repetition (Participant-N) and orange lines showing one *Impaired* repetition (Participant-I). We can observe that the orthosis indeed induced "impaired" motions, i.e., motor strategies that compensate the lack of mobility of the elbow. While lumbar flexion and trunk rotation were nearly absent to perform reaching during the *Natural* repetition (max. -5 and 25 deg resp.), they were important components of the global motion during the *Impaired* repetition (max. -23 and 42 deg resp.). Conversely, shoulder and elbow flexion/extension were importantly reduced during the *Impaired* condition compared to the *Natural* condition (up to -25 deg for shoulder and -40 deg for the elbow). Using lumbar spine and trunk to perform a reaching task when arm mobility is reduced

is typically observed with stroke survivors presenting arm impairment [23]. Looking at the VHT motions generated from the *Impaired* data (VHT-I, blue lines), we see that the reference motion generation algorithm canceled the lumbar flexion (max. -2 deg) and considerably reduced the trunk rotation (max. 24 deg), while restoring shoulder flexion and elbow extension. It can also be noticed that, compared to the *Natural* repetition of the participant, the VHT lumbar flexion was lower and the VHT elbow extended more for the second target to reach (second peak). The VHT motions generated from the *Natural* data (light green, VHT-N) produced even less lumbar and trunk motions than the natural movement of the participant (lumbar flexion close to 0 deg and max. trunk rotation 21 deg), but they produced higher shoulder flexion (up to +15 deg more) and lower elbow flexion (up to -40 deg). The VHT motions generated from the *Natural* condition were similar to those generated from the *Impaired* condition, except a slightly lower trunk rotation (-5 deg) and a higher shoulder flexion (+15 deg). This was expected, as the VHT had the same motor abilities in both conditions.

The tendency observed with the example trajectories was confirmed with the ROM (Fig. 4a): during the *Impaired* repetitions (Participant-I), lumbar and trunk motions were enhanced (+12 deg for lumbar flexion LUMZ, +5 deg for lumbar lateral bending LUMX and +9 deg for trunk rotation TRY) while shoulder and elbow motions were reduced (-17 deg for shoulder flexion SHOZ, -5 deg for shoulder rotation SHOY and -41 deg for elbow flexion ELBZ) compared to the *Natural* repetitions (Participant-N). The VHT motions generated from *Impaired* movements (VHT-I) created very small lumbar and trunk contribution, with ROM very close to natural motions, except for shoulder rotation (SHOY, +12 deg for the VHT) and pronosupination (ELBY, -26 deg for the VHT). The VHT motions generated from the *Natural* condition (VHT-N) produced even lower lumbar and trunk contribution than the genuine participants' natural motions but exhibited more shoulder rotation (+12 deg), more elbow flexion (+13 deg), less pronosupination (-17 deg) and a bit more wrist ulnar deviation (WRX, +6 deg).

To complete this analysis, we used the normalized md-DTW distance to measure the similarity between *Natural* and *Impaired* repetitions of the participants and between participants' *Natural* condition and VHT generated motions. A value of 0 represents perfect matching; the higher the value, the larger the difference between the time series. Individual values (repetitions and participants) are reported in Fig. 4b. The lines connect the mean over the repetitions for each participant. For most participants (6 out of 7), the md-DTW for VHT motions generated from the *Natural* condition was only slightly higher than the one obtained between the benchmark and the *Natural* repetitions of the participants (+0.18 on average). The md-DTW of the VHT motions generated from the *Impaired* repetitions were more disparate and presented higher values than the participants' *Natural* ones (+0.33 on average), but we can observe a decrease of the md-DTW compared to the one of the participants' *Impaired* movements (-0.15 on average).

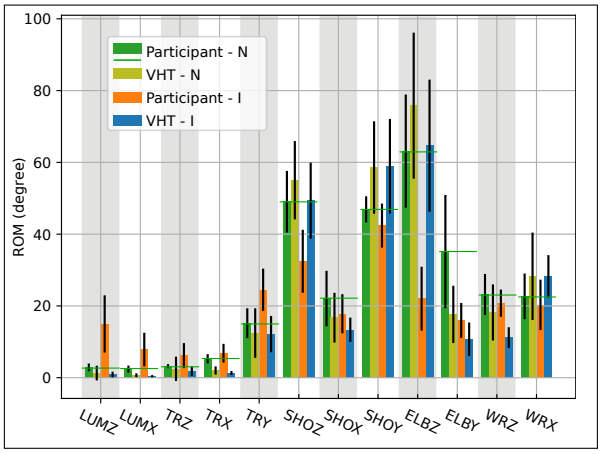

(a) ROM of the joint angles (mean and standard deviation), from the participants and from the VHT, for the two conditions: *Natural* (N) and *Impaired* (I). Values were averaged over repetitions and participants.

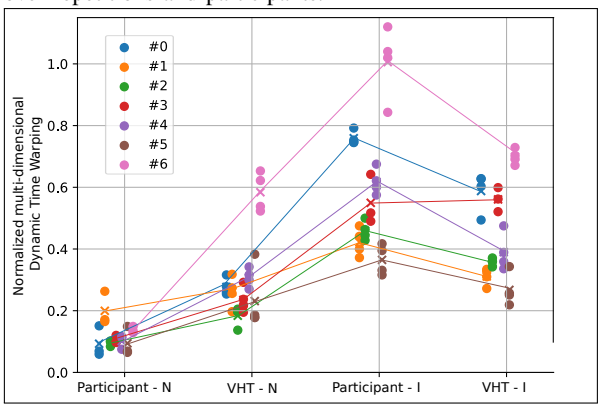

(b) Normalized multi-dimensional DTW distance, with the second *Natural* repetition as benchmark. Participant-N and Participant-I are the results obtained with the recorded data in *Natural* and *Impaired* conditions resp. VHT-N and VHT-I are the results obtained with the motions generated from the *Natural* and *Impaired* conditions resp.

Fig. 4: Reaching task (7 participants): ROM of joint angles and md-DTW distance for participants' motions and VHT (generated) motions, for *Natural* (N) and *Impaired* (I) conditions.

B. Pouring task

To evaluate the capacity of the motion generation algorithm to operate on different tasks, we ran the same analysis with the data of the four participants who performed the pouring task. The execution time of the optimization step for the pouring task was 52±2ms (19Hz). The averaged RMSE of the generated hand pose was 4±0.3mm (*Natural*) and 4±0.5mm (*Impaired*) for the hand marker and 10±1mm (*Natural)* and 10±2mm (*Impaired*) for the two wrist markers. Fig. 5 gathers the ROM and the md-DTW. Fig. 5a shows that the orthosis also induced more lumbar and trunk contribution (+5 deg for trunk lateral bending TRX for instance) with less elbow motion (-10 deg) but also less pronosupination (ELBY, -10 deg) than when the pouring task was performed without

the orthosis. VHT generated motions recovered small lumbar and trunk motions and higher elbow motion, with ROM close to the natural values from participants. However, generated shoulder flexion and rotation (SHOZ and SHOY) tended to have larger ROM than participants' natural motions (+10 deg for shoulder rotation for instance) while generated pronosupination and wrist flexion (WRZ) had smaller ROM (up to -28 deg for pronosupination and -9 deg for wrist flexion for VHT motions generated from the *Impaired* condition). The md-DTW (Fig. 5b) was less variable than for the reaching task: VHT motions generated from the *Natural* condition also had a slightly higher distance with the natural benchmark than participants' natural movements (+0.15 on average), but this was also the case for the participants' pseudo-impaired motions (+0.15 on average). The md-DTW of the VHT motions generated from *Impaired* motions was bigger (+0.27 on average, especially due to the first participant).

V. DISCUSSION AND CONCLUSION

This work presents a novel approach to obtain reference movements (i.e., movements a patient should strive for) for arm movement assessments during motor rehabilitation. This approach aims at providing a seamless and non-task-specific access to patient-tailored reference data, a critical input for objective and detailed motor evaluation. To circumvent a cumbersome data collection requiring time and equipment often unavailable in clinical settings, we suggested to generate reference motions with the VHT, a personalized biomechanical model of the patient.

The VHT and the hand pose of the patient are used to solve an ergonomic optimization problem. To evaluate this approach, we tested the reference motion generation algorithm on two motor tasks, each one involving different joints. Seven unimpaired participants performed a reaching task and four participants a pouring task, naturally and with an orthosis that limited the elbow joint, to mimic motor impairment. With the latter, participants indeed exhibited similar motor strategies to the ones observed for stroke survivors, with a large impact on reaching and a reduced impact on pouring. VHT motions were generated from pseudo-impaired and natural movements of the participants.

Results showed that the VHT indeed managed to follow the hand pose of the participants, while exhibiting realistic joint trajectories with a more ergonomic behavior than participants with orthosis, replacing lumbar and trunk contribution with shoulder and elbow. We could also verify that, when generating motions from natural movements, the VHT motions stayed close to the participants' ones. The VHT motion generation algorithm did not yet exactly reproduce the natural behaviour of the participants. The observed differences can be explained by two main reasons:

- ergonomic power: the VHT motions were too ergonomic, the lumbar spine and the trunk were even less solicited than during participants' natural performance, which led to more elbow extension to reach the targets;
- redundancy of the human body: the swivel angle of the arm was not particularly addressed yet, which led to different contributions of the shoulder, the elbow and the wrist for a same hand pose.

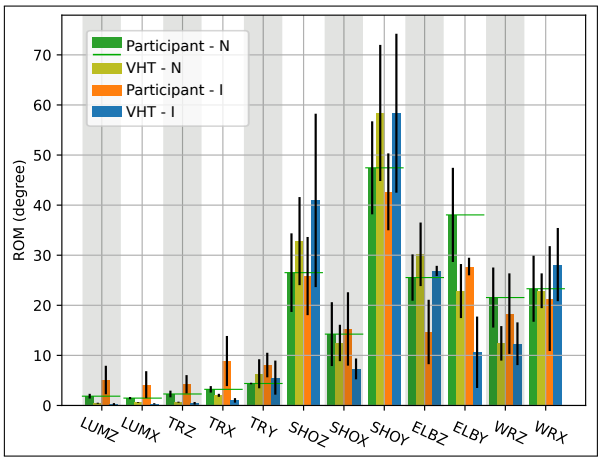

(a) ROM of the joint angles, from the participant and from the VHT, for the two conditions: *Natural* (N) and *Impaired* (I)

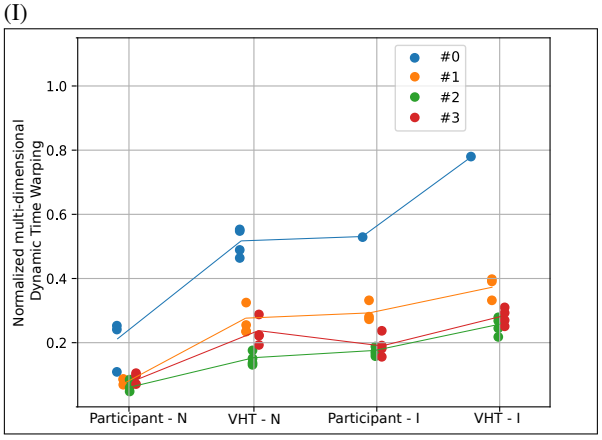

(b) Multi-dimensional DTW with the second natural repetition as reference. Participant-N and Participant-I are the results obtained with the recorded data in *Natural* and *Impaired* conditions resp. VHT-N and VHT-I are the results obtained with the motions generated from the *Natural* and *Impaired* conditions resp.

Fig. 5: Pouring task (4 participants): ROM of joint angles and md-DTW for participants' motions and VHT (generated) motions, for *Natural* (N) and *Impaired* (I) conditions.

Moreover, the reference motion generation depends on the accuracy of the VHT calibration, which is still arduous to perfectly perform with optical motion capture [33]. The discrepancies between the VHT motions and the natural motions of the participants could also be partly explained by an imperfect calibration (i.e., an imperfect matching between the participant's joint centers and the VHT ones), that could be improved with a marker-set more specific to upper-limb than the Plug-in Gait for instance. Optical motion capture is the current gold standard but it would be possible to use markerless motion capture or wearable sensors like inertial measurement units. With its recent progresses, markerless motion capture could be a better candidate to provide the joint center motions than the reconstruction method we used

[34].

The proof-of-concept of generating reference motions based on patient's own movements with the VHT thus showed promise. The VHT approach eliminates the need for several hours of data collection from dozens of unimpaired people for just a single task, which is required to derive the averaged normative data typically used as reference. While data collection with the patient remains necessary, recent advances in markerless motion capture offer the potential to seamlessly integrate this process into clinical practice [35]. Furthermore, by incorporating a kinematic model of the patient, the VHT enables the generation of personalized reference motions that can be adapted to both the patient's morphology and the patient's motor abilities, which is hardly possible with the current approaches. Reference joint trajectories can be generated for completely different motor tasks, with a unique algorithm formulation. To our knowledge, this generality has not been made available or has not been tested so far in methods based on direct or inverse optimal control [17], [22]. Compared to methods with generative models [20], [21], our approach is tailored to the clinical context: it ensures task success, requires no specific GPU and produces the VHT motion in a short time. The short execution time indeed gives the possibility to generate VHT motions in parallel to the patient's performance, with a frequency of approximately 20Hz. This opens promising opportunities for the development of technical supports providing direct information on the performed task, such as real-time augmented feedback [36], [37].

Further developments still need to be conducted to improve the VHT concept until obtaining clinically valid reference motions. First, the issue of redundancy leading to undesired arm swivel angle should be tackled. This could be done by constraining the shoulder, elbow and wrist joints differently with the ergonomic weights in $\mathbf{K}$. These weights could, for instance, be identified with Inverse Reinforcement Learning methods [38], but considering a high number of participants to avoid over-fitting on the training set. With another complementary approach, we could also add the possibility to consider joint synergies in the optimization problem, which could provide a more global resolution than the joint-by-joint approach implemented at the moment, and thus prevent non-natural shoulder-elbow-wrist movements. In this work, we evaluated the VHT motions by comparing them with the participants' unimpaired movements; this evaluation could be completed with a validation by a therapist, to include further clinical considerations. Validation by a therapist will also be particularly relevant when testing the personalization of the VHT motor abilities, i.e. introducing some patient's effective impairments, not yet addressed in this study. When some joints of the VHT are assigned a limited range of motion, comparing the generated reference motions with unimpaired movements will no longer be valid. Finally, additional participants with a wider age range and more diverse morphologies should be included in the validation experiment, together with patients presenting various upper-limb impairments. These next steps will continue building and enhancing the VHT motion generation, opening new perspectives for a straightforward, task-independent and personalized motor assessment.

ACKNOWLEDGMENT

We particularly thank Nicolas Mansard, Vincent Bonnet and Maxime Sabbah from the Gepetto team of the Laboratoire d'Analyse et d'Architecture des Systèmes (LAAS, Toulouse, France), for their support with Pinocchio and the useful discussions. We also thank the participants of the motion data collection.

REFERENCES

[1] F. J. Carod-Artal and J. A. Egido, "Quality of Life after Stroke: The Importance of a Good Recovery," *Cerebrovascular Diseases*, vol. 27, no. Suppl. 1, pp. 204–214, 2009.

[2] A. Schrag, M. Jahanshahi, and N. Quinn, "How does Parkinson's disease affect quality of life? A comparison with quality of life in the general population," *Movement disorders: official journal of the Movement Disorder Society*, vol. 15, no. 6, pp. 1112–1118, 2000.

[3] J. M. Veerbeek, E. van Wegen, R. van Peppen, P. J. Van der Wees, E. Hendriks, M. Rietberg, and G. Kwakkel, "What is the evidence for physical therapy poststroke? A systematic review and meta-analysis," *PloS one*, vol. 9, no. 2, p. e87987, 2014.

[4] S. Mazlan, H. A. Rahman, Y. C. Fai, B. S. K. K. Ibrahim, and M. S. Huq, "Kinematic variables for upper limb rehabilitation robot and correlations with clinical scales: A review," *Bulletin of Electrical Engineering and Informatics*, vol. 9, no. 1, pp. 75–82, 2020.

[5] J. See, L. Dodakian, C. Chou, V. Chan, A. McKenzie, D. J. Reinkensmeyer, and S. C. Cramer, "A standardized approach to the Fugl-Meyer assessment and its implications for clinical trials," *Neurorehabilitation and neural repair*, vol. 27, no. 8, pp. 732–741, 2013.

[6] A. Schwarz, C. M. Kanzler, O. Lambercy, A. R. Luft, and J. M. Veerbeek, "Systematic review on kinematic assessments of upper limb movements after stroke," *Stroke*, vol. 50, no. 3, pp. 718–727, 2019.

[7] A.-M. Hughes, S. B. Bouças, J. H. Burridge, M. Alt Murphy, J. Buurke, P. Feys, V. Klamroth-Marganska, I. Lamers, G. Prange-Lasonder, A. Timmermans *et al.*, "Evaluation of upper extremity neurorehabilitation using technology: a European delphi consensus study within the EU COST Action Network on Robotics for Neurorehabilitation," *Journal of neuroengineering and rehabilitation*, vol. 13, no. 1, p. 86, 2016.

[8] V. Longatelli, D. Torricelli, J. Tornero, A. Pedrocchi, F. Molteni, J. L. Pons, and M. Gandolla, "A unified scheme for the benchmarking of upper limb functions in neurological disorders," *Journal of neuroengineering and rehabilitation*, vol. 19, no. 1, p. 102, 2022.

[9] T. Weikert, Y. Li, D. Paez-Granados, and C. A. Easthope, "Automated prediction of item-level ARAT scores from wearable sensors," in *2025 International Conference On Rehabilitation Robotics (ICORR)*. IEEE, 2025, pp. 1239–1244.

[10] R. Yang, A. Kennedy, and R. J. Cotton, "BiomechGPT: Towards a biomechanically fluent multimodal foundation model for clinically relevant motion tasks," *arXiv preprint arXiv:2505.18465*, 2025.

[11] R. Baptista, E. Ghorbel, A. E. R. Shabayek, F. Moissenet, D. Aouada, A. Douchet, M. André, J. Pager, and S. Bouilland, "Home self-training: Visual feedback for assisting physical activity for stroke survivors," *Computer Methods and Programs in Biomedicine*, vol. 176, pp. 111–120, jul 2019.

[12] A. Merlo, M. Longhi, E. Giannotti, P. Prati, M. Giacobbi, E. Ruscelli, A. Mancini, M. Ottaviani, L. Montanari, and D. Mazzoli, "Upper limb evaluation with robotic exoskeleton. normative values for indices of accuracy, speed and smoothness," *NeuroRehabilitation*, vol. 33, no. 4, pp. 523–530, 2013.

[13] D. B. Chaffin, J. J. Faraway, X. Zhang, and C. Woolley, "Stature, age, and gender effects on reach motion postures," *Human factors*, vol. 42, no. 3, pp. 408–420, 2000.

[14] P. Buckle and J. Buckle, "Obesity, ergonomics and public health," *Perspectives in public health*, vol. 131, no. 4, pp. 170–176, 2011.

[15] A. W. Andrews and R. W. Bohannon, "Decreased shoulder range of motion on paretic side after stroke," *Physical Therapy*, vol. 69, no. 9, pp. 768–772, 1989.

[16] L. A. Ingram, A. A. Butler, M. A. Brodie, S. R. Lord, and S. C. Gandevia, "Quantifying upper limb motor impairment in chronic stroke: a physiological profiling approach," *Journal of Applied Physiology*, vol. 131, no. 3, pp. 949–965, 2021.

[17] B. Berret, C. Darlot, F. Jean, T. Pozzo, C. Papaxanthis, and J. P. Gauthier, "The inactivation principle: mathematical solutions minimizing the absolute work and biological implications for the planning of arm movements," *PLoS computational biology*, vol. 4, no. 10, 2008.

[18] S. Ivaldi, O. Sigaud, B. Berret, and F. Nori, "From humans to humanoids: the optimal control framework," *Paladyn, Journal of Behavioral Robotics*, vol. 3, no. 2, pp. 75–91, 2012.

[19] S. L. Delp, F. C. Anderson, A. S. Arnold, P. Loan, A. Habib, C. T. John, E. Guendelman, and D. G. Thelen, "OpenSim: open-source software to create and analyze dynamic simulations of movement," *IEEE transactions on biomedical engineering*, vol. 54, no. 11, pp. 1940–1950, 2007.

[20] A. Khani, A. Rampini, B. Roy, L. Nadela, N. Kaplan, E. Atherton, D. Cheung, and J. Bibliowicz, "Motion Generation: A survey of generative approaches and benchmarks," *arXiv preprint arXiv:2507.05419*, 2025.

[21] X. Huang, T. Truong, Y. Zhang, F. Yu, J. P. Sleiman, J. Hodgins, K. Sreenath, and F. Farshidian, "Diffuse-cloc: Guided diffusion for physics-based character look-ahead control," *ACM Transactions on Graphics (TOG)*, vol. 44, no. 4, pp. 1–12, 2025.

[22] J. F.-S. Lin, P. Carreno-Medrano, M. Parsapour, M. Sakr, and D. Kulić, "Objective learning from human demonstrations," *Annual Reviews in Control*, vol. 51, pp. 111–129, 2021.

[23] M. Cirstea and M. F. Levin, "Compensatory strategies for reaching in stroke," *Brain*, vol. 123, no. 5, pp. 940–953, 2000.

[24] A. Touillet, A. Gouzien, M. Badin, P. Herbe, N. Martinet, N. Jarrassé, and A. Roby-Brami, "Kinematic analysis of impairments and compensatory motor behavior during prosthetic grasping in below-elbow amputees," *PLoS One*, vol. 17, no. 11, 2022.

[25] A. Poignant, M. Legrand, N. Jarrassé, and G. Morel, "Computing the positioning error of an upper-arm robotic prosthesis from the observation of its wearer's posture," in *2021 IEEE International Conference on Robotics and Automation (ICRA)*, 2021.

[26] L. McAtamney and N. Corlett, "Rapid upper limb assessment (rula)," in *Handbook of human factors and ergonomics methods*. CRC Press, 2004, pp. 86–96.

[27] *Plug-In Gait Reference Guide*. Vicon Motion Systems Limited, 2020.

[28] T. Giorgino, "Computing and visualizing dynamic time warping alignments in R: the dtw package," *Journal of statistical Software*, vol. 31, pp. 1–24, 2009.

[29] P. Tormene, T. Giorgino, S. Quaglini, and M. Stefanelli, "Matching incomplete time series with dynamic time warping: an algorithm and an application to post-stroke rehabilitation," *Artificial intelligence in medicine*, vol. 45, no. 1, pp. 11–34, 2009.

[30] M. Shokoohi-Yekta, B. Hu, H. Jin, J. Wang, and E. Keogh, "Generalizing dynamic time warping to the multi-dimensional case requires an adaptive approach." SDM, 2015.

[31] J. Carpentier, G. Saurel, G. Buondonno, J. Mirabel, F. Lamiraux, O. Stasse, and N. Mansard, "The Pinocchio C++ library: A fast and flexible implementation of rigid body dynamics algorithms and their analytical derivatives," in *2019 IEEE/SICE International Symposium on System Integration (SII)*. IEEE, 2019, pp. 614–619.

[32] J. A. Andersson, J. Gillis, G. Horn, J. B. Rawlings, and M. Diehl, "CasADi: a software framework for nonlinear optimization and optimal control," *Mathematical Programming Computation*, vol. 11, no. 1, pp. 1–36, 2019.

[33] J. F. O'Brien, R. E. Bodenheimer, G. J. Brostow, and J. K. Hodgins, "Automatic joint parameter estimation from magnetic motion capture data," *arXiv preprint arXiv:2303.10532*, 2023.

[34] T. Unger, A. S. Moslehian, J. Peiffer, J. Ullrich, R. Gassert, O. Lambercy, R. J. Cotton, and C. A. Easthope, "Differentiable biomechanics for markerless motion capture in upper limb stroke rehabilitation: A comparison with optical motion capture," *IEEE Transactions on Medical Robotics and Bionics*, 2025.

[35] R. M. Hansen, S. L. Arena, and R. M. Queen, "Validation of upper extremity kinematics using markerless motion capture," *Biomedical Engineering Advances*, vol. 7, p. 100128, 2024.

[36] M. Cirstea and M. F. Levin, "Improvement of arm movement patterns and endpoint control depends on type of feedback during practice in stroke survivors," *Neurorehabilitation and neural repair*, vol. 21, no. 5, pp. 398–411, 2007.

[37] M. Legrand-Lestoille, F. Grenet, O. Hochstrasser, A. Luft, R. Gassert, O. Lambercy, and C. E. Awai, "Real-time augmented feedback for gait training: are gait responses affected by the choice of target parameter?" *Frontiers in Bioengineering and Biotechnology*, vol. 13, 2025.

[38] S. Adams, T. Cody, and P. A. Beling, "A survey of inverse reinforcement learning," *Artificial Intelligence Review*, vol. 55, no. 6, pp. 4307–4346, 2022.